American Mineralogist, Volume 95, pages 487–494, 2010

Arsenic-rich fergusonite-beta-(Y) from Mount Cervandone (Western Alps, Italy): Crystal structure and genetic implications

Alessandro Guastoni,[1] Fernando Cámara,[2] and Fabrizio Nestola[1,3,*]

[1]Department of Geoscience, University of Padova, via Giotto 1, 35137 Padova, Italy
[2]CNR-Institute of Geosciences and Georesources, U.O.S. Pavia, via Ferrata 1, 27100 Pavia, Italy
[3]CNR-Institute of Geosciences and Georesources, U.O.S. Padova, via Giotto 1, 35137 Padova, Italy

Abstract

An As-rich variety of fergusonite-beta-(Y) occurs as greenish yellow pseudo-bipyramidal crystals up to 1 mm in length in centimeter-sized secondary cavities within sub-horizontal pegmatite dikes at Mount Cervandone (Western Alps, Italy). The mineral is associated with quartz, biotite, potassium feldspar, and orange-yellow barrel-shaped hexagonal crystals of synchysite-(Ce) up to 2 mm in length. Fergusonite-beta-(Y) crystallized during the Alpine metamorphism under amphibolite-facies conditions, as a result of interaction between As-enriched hydrothermal fluids, circulating through the pegmatite dikes, and precursor accessory minerals in the pegmatites enriched in high-field-strength elements. These pegmatites are of NYF (niobium-yttrium-fluorine) geochemical type and served as the principal source of Be, Y, Nb, Ta, and rare-earth elements (REE) that were liberated and redeposited as rare Be-As-Y-REE minerals, including the As-rich fergusonite-beta-(Y). The latter mineral crystallizes with monoclinic symmetry [a = 5.1794(14), b = 11.089(3), c = 5.1176(14) Å, β = 91.282(8)°, V = 293.87(14) Å^3, space group $I2/a$] and has the empirical formula $(Y_{0.70}Dy_{0.07}Er_{0.05}Ca_{0.05}Gd_{0.02}U_{0.02}Yb_{0.01}Tb_{0.01}Th_{0.01}Nd_{0.01})_{\Sigma 0.95}(Nb_{0.68}As^{5+}_{0.27}W_{0.06}Ta_{0.01}Si_{0.01})_{\Sigma 1.03}O_4$. The crystal structure of fergusonite-beta-(Y) has been refined using a thermally untreated single crystal to R_1 = 6.6% for 441 observed reflections with $F_o/\sigma F_o > 4$. The incorporation of As in the structure of monoclinic fergusonite-type phases is discussed in the context of the data available for synthetic analogs.

Keywords: Fergusonite, single crystal, X-ray diffraction, EMPA

Introduction and previous work

The compound $YNbO_4$ (fergusonite) occurs as different polymorphs depending on the temperature of crystallization (Wolten 1967): a high-T polymorph (space group $I4_1/a$, no. 88, Z = 4) isostructural with scheelite ($CaWO_4$; Hazen et al. 1985) and powellite ($CaMoO_4$; Crichton and Grzechnik 2004); and a low-T polymorph with the fergusonite-type structure (known also in the mineralogical literature as fergusonite-beta, space group $I2/a$, no. 15, Z = 4). The structures of both scheelite- and fergusonite-type polymorphs were first determined by Komkov (1959), who proposed the non-centrosymmetric space group $I2$ for the fergusonite type. This author observed the monoclinic polymorph after annealing a natural tetragonal fergusonite crystal at 1000 °C for 15 min. Neutron diffraction studies of synthetic $YNbO_4$ have shown that it actually crystallizes with space group $I2/a$ (no. 15, Weitzel and Schröcke 1980). The standard setting for space group $I2/a$ is $C2/c$, which can be obtained from the former by applying the transformation matrix $(00\bar{1}/010/101)$. However, to facilitate comparison with the scheelite-type structure, we will use the body-centered setting in the present work. Wolten and Chase (1967) observed in synthetic $YTaO_4$ that the low-T fergusonite-type structure forms only as a consequence of a displacive second-order transformation of the scheelite-type structure. For the same compound, a different monoclinic polymorph (space group $P2/a$, no. 13, Z = 2) forms at T above the tetragonal-monoclinic transition and transforms very slowly on cooling to a scheelite-type structure through a discontinuous transition. Sugitani and Nagashima (1975) claimed to have observed the $P2/a$ monoclinic structure also in synthetic $YNbO_4$. Recently, Hori et al. (2006) have described the natural occurrence of $YTaO_4$, approved as the new mineral iwashiroite-(Y), whose structure has the same topology as wolframite (space group $P2/c$, no. 13, with Z = 2). Due to the structural similarity between iwashiroite-(Y) and wolframite and the extensive Nb for Ta substitution in iwashiroite-(Y), the existence of a wolframite-type phase is expected also for $YNbO_4$.

The stoichiometry of the above-mentioned three polymorphs is of type ABX_4, where the B sites are fourfold coordinated and the A sites are eightfold coordinated. However, these three polymorphs are not the only possible topologies for ABX_4 compounds with B = (Nb,Ta) and X = O. If A = Sb^{3+} or Bi^{3+}, the structure is orthorhombic and can be either polar (space group $Pc2_1n$) or centrosymmetric ($Pcnn$), as seen in the stibiotantalite-stibiocolumbite and bismutotantalite-bismutocolumbite series (Galliski et al. 2001 and references therein). Even though the charge distribution and lattice parameters of these phases are similar to fergusonite (A = R^{3+}, B = R^{5+}), the topologies of these minerals are completely different because in the Sb and Bi oxides, both A and B sites are sixfold coordinated. A different, yet monoclinic, polymorph has been described at high P for $BaWO_4$ ($BaWO_4$-II type, space group $P2_1/n$, no. 14, Z = 8),

* E-mail: fabrizio.nestola@unipd.it

which has the scheelite structure at room *P* (see Manjon and Errandonea 2009, for a review of high-*P* transformations in the ABX_4 compounds). Last, if Nb occupies the A site and boron the B site (as in behierite, $NbBO_4$), the symmetry becomes $I4_1/amd$ (no. 141, $Z = 4$) corresponding to a zircon-type structure topology (e.g. Mrose and Rose 1961). In fact, members of the solid solution between xenotime-(Y) (YPO_4; Krstanović 1965) and chernovite-(Y) ($YAsO_4$; Goldin et al. 1967), which also preserve the same stoichiometry and charge distribution, also crystallize with the zircon-type structure and can transform to a scheelite-type structure at high *P* (Zhang et al. 2008). Phosphates and arsenates of rare-earth elements (REE) with ABX_4 stoichiometry also occur as monoclinic monazite-type structures (space group $P2_1/n$, no. 14, $Z = 4$).

Unit-cell data for an unheated sample of fergusonite-type $YNbO_4$ from granitic pegmatites at Batou, Inner Mongolia, were first reported by Gorzhevskaya et al. (1961). The Ce-dominant fergusonite-type $CeNbO_4$, formerly known as brocenite, from the Chernigovskiy carbonatite in Ukraine, upon heating to 700 °C gave an X-ray pattern identical to that of synthetic $CeNbO_4$, $NdNbO_4$, and $PrNbO_4$ (Chashka and Marchenko 1976). A survey of the literature shows that no crystal structure refinements of natural fergusonite-type $YNbO_4$ have been published so far. The structure topology of the fergusonite-type structure has recently attracted interest because it is characteristic of stable high-pressure polymorphs of ABX_4 compounds with the scheelite structure. Materials with the ABX_4 stoichiometry are of technological importance as solid-state lasers (X = F), solid-state scintillators (X = O) (Errandonea et al. 2005, 2008 and references therein), and super-hard materials (e.g., reidite, $ZrSiO_4$, Reid and Ringwood 1969; Liu 1979; Scott et al. 2002). Recently, a fergusonite-type structure has been observed for a quenched high-*P* phase of $(Zr,Ti)O_2$ (Troitzsch et al. 2007), which is used as a temperature-stable dielectric material in ceramic capacitors and as a stable oscillator at microwave frequencies in satellite communication.

The present study is the first report of the crystal structure of unheated naturally occurring fergusonite-type $YNbO_4$, as exemplified by As-rich fergusonite-beta-(Y) from Mount Cervandone (Verbano-Cusio-Ossola, Devero valley, Western Alps, Italy). We also provide the first description of the crystal chemistry of an As-rich fergusonite-group mineral. Mount Cervandone and the Swiss Wannigletscher (also referred to as Cherbadung) are among the best-known mineral localities in the Alps. A plethora of rare minerals from this locality has been investigated in detail (Graeser and Albertini 1995), including several arsenate minerals that were discovered here: asbecasite $[Ca_3(Ti,Sn^{4+})As_6^{3+}Si_2Be_2O_{20}]$ and cafarsite $[Ca_8(Ti,Fe^{2+},Fe^{3+},Mn)_{6-7}(As^{3+}O_3)_{12}\cdot 4H_2O]$ (Graeser 1966); cervandonite-(Ce) $[(Ce,Nd,La)(Fe^{3+},Fe^{2+},Ti^{4+},Al)_3O_2(Si_2O_7)_{1-x+y}(AsO_3)_{1+x-y}(OH)_{3x-3y}]$ (Demartin and Gramaccioli 2008); fetiasite $[(Fe^{2+},Fe^{3+},Ti)_3O_2(As_2^{3+}O_5)]$ (Graeser et al. 1994); gasparite-(Ce) $[(Ce,La,Nd)AsO_4]$ (Graeser and Schwander 1987); and paraniite-(Y) $[Ca_2Y(AsO_4)(WO_4)_2]$ (Demartin et al. 1994).

Occurrence and description of the paragenesis

As-rich fergusonite-beta-(Y) from Mount Cervandone occurs as pseudo-bipyramidal crystals up to 1 mm in length (Fig. 1), which have a greenish yellow color under incandescent light and yellow color under sunlight. The mineral occurs in centimeter-sized secondary cavities hosted by sub-horizontal pegmatite dikes, and is associated with quartz, biotite, potassium feldspar, and orange-yellow barrel-shape hexagonal crystals of synchysite-(Ce) up to 2 mm in length. The Mount Cervandone locality was previously described as a typical example of Alpine-type quartz-bearing fissures (Graeser and Albertini 1995). However, recent studies indicate that the mineralized fissures of Mount Cervandone and Wannigletscher are mainly found in, and related to, pegmatitic dikes (Guastoni et al. 2006). These dikes are strongly deformed and contorted, exhibiting boudinage-like textures, but they are generally concordant with the foliation of fine-grained two-mica leucocratic gneiss, which can be interpreted as leucogranitic-aplitic rocks metamorphosed under amphibolite-facies conditions (Dal Piaz 1975). The dikes have a thickness of several decimeters and are composed of coarse vitreous and smoky quartz, potassium feldspar, and greenish micas (probably muscovite). Locally, the pegmatite dikes are crosscut by Alpine-type quartz veins, which are generally subvertical, discordant with respect to the foliation of the gneissic host rocks and commonly contain open fissures lined with quartz crystals. Several accessory minerals are found in these quartz fissures, including cafarsite, agardite-(Y), asbecasite, chernovite-(Y), gasparite-(Ce), rutile, anatase, and tennantite. The latter sulfide mineral is frequently associated with several arsenates, carbonates, sulfates, and vanadates of Fe, Cu, Pb, and Zn (Guastoni et al. 2006).

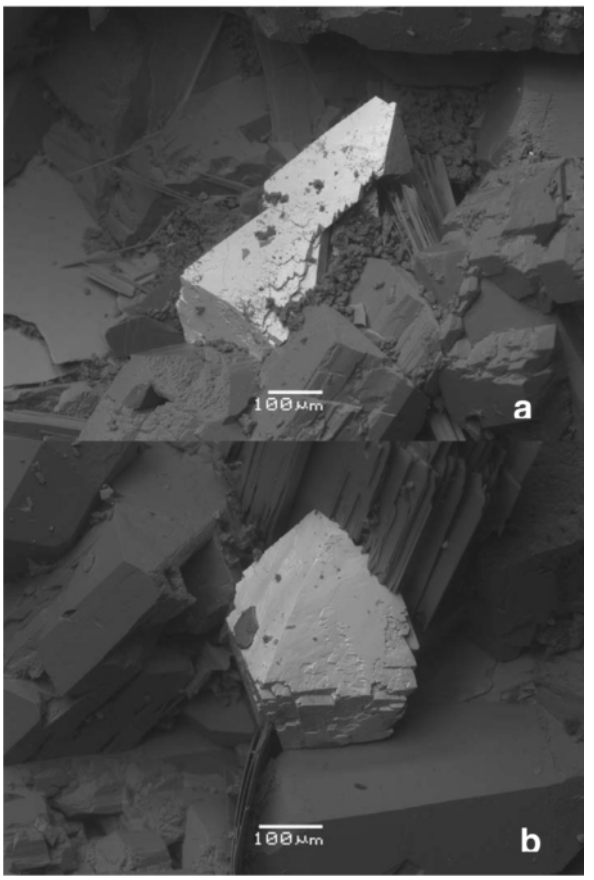

Figure 1. Secondary-electron image of two pseudo-bipyramidal crystals of As-rich fergusonite-beta-(Y) from Mount Cervandone.

The pegmatite dikes show a strong NYF (niobium-yttrium-fluorine) geochemical signature manifested in the presence of several Be-As-Nb-Y rare-earth minerals, which include aeschynite-(Y), agardite-(Y), Nb-rich anatase, asbecasite, cervandonite-(Ce), chernovite-(Y), crichtonite-group minerals, As-rich fergusonite-beta-(Y), fluorite, gadolinite-(Y), monazite-(Ce), paraniite-(Y), Nb-rich rutile, synchysite-(Ce), and xenotime-(Y). The assemblages of arsenates, carbonates, sulfates, and vanadates of Fe, Cu, Pb, and Zn are mainly hosted by quartz veins deposited by hydrothermal fluids during the Alpine event. We interpret these assemblages as products of crystallization from As-enriched hydrothermal fluids generated during the Alpine metamorphism under amphibolite-facies conditions. Interaction of the fluids circulating through the pegmatite dikes with the aforementioned accessory minerals enriched in high-field-strength elements resulted in the breakdown of these minerals, remobilization of Be, Y, Nb, Ta, and REE, and crystallization of several rare Be-As-Y-REE minerals, including the As-rich variety of fergusonite-beta-(Y) studied in the present work.

Analytical methods

The chemical composition of As-rich fergusonite-beta-(Y) was determined using a Cameca-Camebax SX50 electron microprobe operating in wavelength-dispersive mode with a focused beam (~1 µm in diameter), an acceleration voltage of 20 kV, and a beam current of 20 nA, with 10 and 5 s counting times for peak and background, respectively. X-ray counts were converted to oxide wt% using the PAP correction program supplied by Cameca (Pouchou and Pichoir 1985). The following natural and synthetic standards, spectral lines and detector types were used in the analysis: wollastonite (Si*K*α, Ca*K*α, TAP), corundum (Al*K*α, TAP), apatite (P*K*α, TAP), Fe_2O_3 (Fe*K*α, LiF), AsGa (As*L*α, TAP), Zr-Y-REE-silicates (Zr*L*α, Y*L*α, REE*L*α, and Nd*L*β, LiF), synthetic UO_2 and ThO_2 (U*M*α and Th*M*α, PET), metallic Nb (Nb*L*α, PET), and Ta and W (Ta*L*α and W*L*α, LiF). The concentrations of Al, P, Fe, and Zr were found to be below the detection limit of the electron microprobe (ca. 0.05 wt%). The average composition and formula of fergusonite-beta-(Y) are reported in Table 1.

Diffraction data were obtained from a very small single crystal (0.13 × 0.10 × 0.07 mm^3) mounted on a Bruker AXS SMART APEX diffractometer equipped with a graphite-filtered Mo*K*α X-ray source and a CCD detector. Despite the small size of the sample, the diffraction spots showed a significant mosaicity. The intensities of 3053 reflections with $-8 < h < 8$, $-17 < k < 17$, $-8 < l < 8$ were collected to 70 °2θ with an acquisition time of 15 s per 0.2° frame. An empirical absorption correction (SADABS, Sheldrick 1998) was applied to the acquired data. The refined unit-cell parameters (Table 2) were obtained from 928 reflections. On the basis of 441 unique observed reflections ($F_o > 4\sigma F$), the crystal structure was refined in space group *I*2/*a* (no. 15, setting b3), starting from the coordinates of Santoro et al. (1980), transformed for this setting with the SHELXL 97 program (Sheldrick 1997) using the WinGX integrated system (Farrugia 1999) to R_1 = 6.6% and a goodness-of-fit value of 1.16. Scattering curves for ionized atoms were taken from the *International Tables for Crystallography* (Wilson 1992). The *R* indices and all other pertinent details of the refinement are summarized in Table 2. Site occupancies for the A and B sites were refined with the scattering curves of Dy and Nb, respectively. The chemical analysis (Table 1) obtained from the same crystal indicates that X-ray scattering at the A site is significantly higher than that from Y. Accordingly, we decided to use the scattering factor of the stronger scatterer Dy, which has an ionic radius similar to that of Y. Agreement between observed (X-ray) and calculated (i.e., based on the electron microprobe analysis) scattering per site is satisfactory (Table 1). Final atomic parameters are given in Table 3, and selected atomic distances and angles in Table 4. A table of observed and calculated structure factors is available from the authors upon request.

Table 1. Average composition of As-rich fergusonite-beta-(Y) from Mount Cervandone and formula calculated on the basis of 4 O atoms

Oxide	wt%	Range	Element	apfu
SiO_2	0.17	0.09–0.25	Si	0.007
As_2O_5	12.05	10.19–16.15	W^{6+}	0.056
Ta_2O_5	0.71	30.31–37.38	As^{5+}	0.270
Nb_2O_5	35.23	0.51–1.18	Ta^{5+}	0.008
WO_3	5.04	4.24–6.70	Nb^{5+}	0.683
Ce_2O_3	0.21	0.06–0.38	ΣB	1.024
Nd_2O_3	0.41	0.17–0.51		
Sm_2O_3	0.16	0.10–0.45	Y	0.702
Gd_2O_3	1.66	1.52–1.91	Ca	0.046
Tb_2O_3	0.59	0.38–0.73	Ce	0.003
Dy_2O_3	5.01	4.73–5.20	Nd	0.006
Er_2O_3	3.61	3.32–3.83	Sm	0.002
Yb_2O_3	0.90	0.55–1.30	Gd	0.024
ThO_2	0.58	0.45–0.66	Tb	0.008
UO_2	2.28	1.51–3.23	Dy	0.069
Y_2O_3	30.79	29.45–31.50	Er	0.049
CaO	1.01	0.81–1.15	Yb	0.012
Total	100.41		Th	0.006
			U	0.022
s.s. B_{calc}	41.75		ΣA	0.949
s.s. A_{calc}	42.29			
s.s. B_{obs}	41.82	ΔB (%)	−0.1	
s.s. A_{obs}	41.51	ΔA (%)	1.8	

Note: s.s. obs is the observed site scattering obtained from the refinement of the crystal structure, here reported in electrons per formula unit (epfu); s.s. calc is the site scattering calculated from the chemical composition obtained by electron-microprobe analysis.

Results and discussion

Composition

Back-scattered electron images (BSE) of polished fragments of the As-rich fergusonite-beta-(Y) crystal used for the structure refinement show that it is devoid of zoning and does not contain any exsolved phases (Fig. 2a). However, the electron microprobe analyses (Table 1) indicate significant variations in the occupancy of the B site: 30.31–37.38 wt% Nb_2O_5, 10.19–16.15 wt% As_2O_5, 4.24–6.70 wt% WO_3, and 0.51–1.18 wt% Ta_2O_5. From Figure 2b, it is clear that the highest (Nb+Ta) contents (0.704–0.748 atoms per formula unit, apfu) are found at the core, whereas the highest As contents (0.300–0.394 apfu) are confined to the rim of the crystal. The W content is almost constant across the crystal, and As is never a dominant species at the B site. At the A site, the mineral shows a more homogeneous composition (Table 1) dominated by Y and heavy REE.

Table 2. Crystal data and structure refinement details for As-rich fergusonite-beta-(Y)

Formula weight	960.34	
Temperature	298(2) K	
Wavelength	0.71073 Å	
Crystal system	Monoclinic	
Space group	*I*2/*a*	
Unit-cell dimensions	*a* = 5.1794(14) Å	α = 90°
	b = 11.089(3) Å	β = 91.282(8)°
	c = 5.1176(14) Å	γ = 90°
Volume	293.87(14) $Å^3$	
Z	8	
Density (calculated)	5.427 Mg/m^3	
Absorption coefficient	26.250 mm^{-1}	
F(000)	432	
Crystal size	0.13 × 0.10 × 0.07 mm^3	
Theta range for data collection	3.67 to 35.15°	
Index ranges	$-8 \leftarrow h \leftarrow 8$, $-17 \leftarrow k \leftarrow 17$, $-8 \leftarrow l \leftarrow 8$	
Reflections collected	3053	
Independent reflections	655 (R_{int} = 0.0469)	
Completeness to theta = 35.15°	99.7%	
Absorption correction	Semi-empirical from equivalents	
Max. and min. transmission	0.160 and 0.080	
Refinement method	Full-matrix least-squares on F^2	
Data / restraints / parameters	655 / 0 / 31	
Goodness-of-fit on F^2	1.157	
Final *R* indices [$I > 2\sigma(I)$]	*R*1 = 0.0663, *wR*2 = 0.2019	
R indices (all data)	*R*1 = 0.0874, *wR*2 = 0.2189	
Largest diff. peak and hole	5.139 and −1.495 e·$Å^{-3}$	

TABLE 3. Atomic coordinates and equivalent isotropic displacement parameters (Å^2 × 10^3) for As-rich fergusonite-beta-(Y)

Atom	Wyck	Occ.*	*x*	*y*	*z*	U_{eq}	U_{11}	U_{22}	U_{33}	U_{23}	U_{13}	U_{12}
A	4*e*	41.51	¼	0.1244(1)	0	23(1)	27(1)	14(1)	27(1)	0	−1(1)	0
B	4*e*	41.82	¼	0.6302(1)	0	25(1)	21(1)	33(1)	20(1)	0	1(1)	0
O1	8*f*		0.0039(16)	0.7108(7)	0.1760(20)	43(3)	39(5)	25(4)	66(6)	10(4)	2(4)	4(3)
O2	8*f*		0.9105(16)	0.4580(6)	0.2508(15)	32(2)	35(4)	21(3)	41(4)	1(3)	−4(3)	4(3)

Notes: U_{eq} is defined as one third of the trace of the orthogonalized U_{ij} tensor. The anisotropic displacement factor exponent takes the form: $-2\pi^2[h^2a^{*2}U_{11} + ... + 2hka^*b^*U_{12}]$.
* Occupancies obtained using the scattering curves of Dy and Nb at the A and B sites, respectively.

TABLE 4. Selected distances and angles for As-rich fergusonite-beta-(Y)

A-O2 (×2)	2.335(8)
A-O2 (×2)	2.402(7)
A-O1 (×2)	2.344(9)
A-O1 (×2)	2.414(8)
<A-O>	2.374
V_A (Å^3)	23.56
A-B	3.600(1)
A-A	3.783(1)
B-O2 (×2)	1.802(8)
B-O1 (×2)	1.813(9)
<B-O>	1.807
V_B (Å^3)	2.98
AV*	46.8
QE*	1.0123
O1-B-O1	120.9(5)
O2-B-O2	114.2(4)
O1-B-O2 (×2)	107.6(4)
O1-B-O2 (×2)	103.4(4)
O2-A-O2	133.9(4)
O1-A-O1	131.8(4)
O1-A-O1	81.6(4)
O2-A-O2	79.6(4)
O2-A-O1 (×2)	101.6(3)
O2-A-O1 (×2)	96.8(3)
O2-A-O2 (×2)	71.02(17)
O2-A-O2 (×2)	74.0(3)
O1-A-O2 (×2)	153.6(3)
O1-A-O2 (×2)	74.5(3)
O2-A-O1 (×2)	153.8(3)
O2-A-O1 (×2)	72.3(2)
O1-A-O1 (×2)	74.7(3)
O1-A-O1 (×2)	69.21(19)
O2-A-O1 (×2)	126.0(3)
O2-A-O1 (×2)	125.1(3)

*AV = angle variance, QE = quadratic elongation (Robinson et al. 1971).

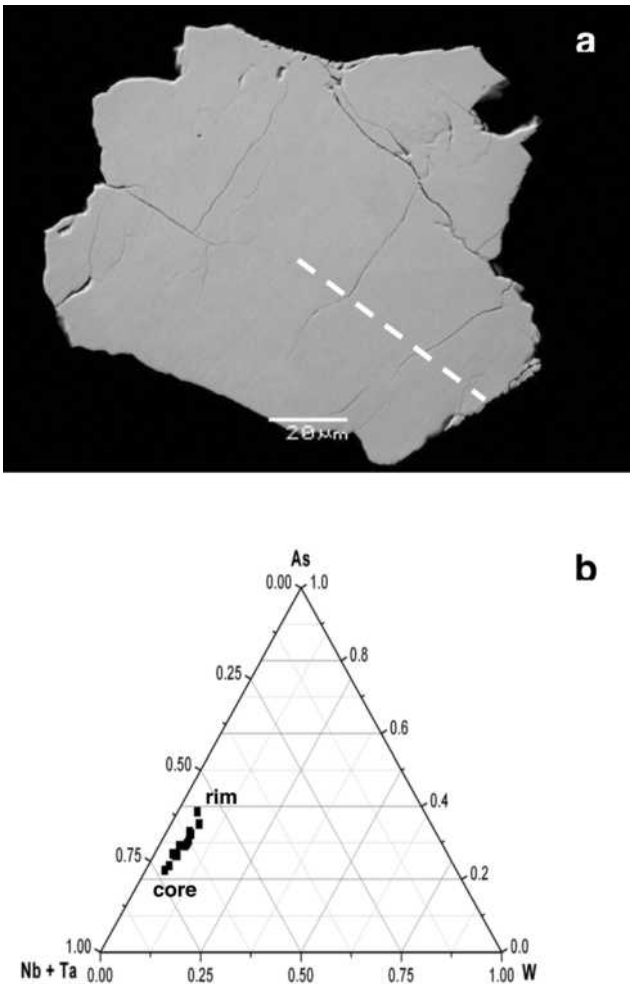

FIGURE 2. Back-scattered electron image of the studied crystal (**a**) showing the location of electron-microprobe analyses plotted in **b**, in terms of the main constituents at the B site.

Crystal structure

The observed site scattering value at the B site agrees well with the average value obtained from the chemical composition. The substitution of As for Nb in the B site reduces the average observed <B-O> distance from 1.883 Å in synthetic fergusonite-type $REENbO_4$ compounds to 1.808 Å in the Mount Cervandone sample (Table 5). Complete substitution of Nb with As in the B site would lead to a <B-O> distance of 1.740 Å observed in chernovite-(Y) (Strada and Schwendimann 1934). At the same time, this substitution reduces deformation of the B-site geometry from an angle-variance (AV, Robinson et al. 1971) value of 141.4 to 46.9 for fergusonite-type $ErNbO_4$ (Keller 1962) and the studied sample, respectively. In the scheelite-type structure, AV values are in the range 22.4–26.14 (see Table 5). Nonetheless, in the zircon-type structure of chernovite-(Y), the AsO_4 tetrahedron is highly deformed. An increase in As content is probably also responsible for the reduction of the β angle from 94.6 to 91.3° from $REENbO_4$ compounds to As-rich fergusonite-beta-(Y), respectively (see Table 5). Interestingly, the compound $BiAsO_4$, which can crystallize with both the scheelite-type structure (tetraroosevelite, Mooney 1948) and the monazite-type structure (rooseveltite, Bedlivy and Mereiter 1982), show smaller <As-O> distances of 1.619 and 1.682 Å, respectively. The structure of synthetic $SmAsO_4$ has been recently reported to also have a scheelite-type structure (Kang and Schleid 2006) and shows <As-O> = 1.697 Å. The difference in the observed <As-O> distances between $SmAsO_4$ and tetraroosevelite may be due to the lower quality of structural data available for the latter. The AV value of rooseveltite (54.68) is closer to that observed in the studied crystal.

In the literature, there is a significant volume of crystallo-

TABLE 5. Selected average bond distances, distortion parameters, average ionic radii (<r_i>), and lattice parameters of ABX_4 compounds with A = REE, B = Nb or As, and X = O

Structure type	ABX_4	<A-O> (Å)	<B-O> (Å)	AV*	QE*	^{A}<r_i> (Å)	^{B}<r_i> (Å)	*a* (Å)	*b* (Å)	*c*† (Å)	β (°)	(*a*+*c*)/2 (Å)	Ref.
Fergusonite-type	$LuNbO_4$	2.321	1.886	120.91	1.033	0.977	0.48	5.229(3)	10.822(8)	5.042(2)	94.38(2)	5.136	1
Fergusonite-type	$YbNbO_4$	2.329	1.877	128.43	1.034	0.985	0.48	5.239(1)	10.834(1)	5.044(1)	94.47(1)	5.142	2
Fergusonite-type	$TmNbO_4$	2.331	1.894	119.83	1.033	0.994	0.48	5.262(2)	10.876(5)	5.049(2)	94.52(5)	5.156	1
Fergusonite-type	$ErNbO_4$	2.346	1.888	141.40	1.036	1.004	0.48	5.280(1)	10.916(5)	5.064(2)	94.48(8)	5.172	1
Fergusonite-type	$HoNbO_4$	2.358	1.880	129.47	1.035	1.015	0.48	5.299(1)	10.947(1)	5.072(1)	94.53(1)	5.185	2
Fergusonite-type	$YNbO_4$	2.363	1.894	121.79	1.035	1.019	0.48	5.317(1)	10.999(1)	5.090(1)	94.53(1)	5.204	3
Fergusonite-type	$DyNbO_4$	2.360	1.899	139.40	1.036	1.027	0.48	5.320(1)	11.000(8)	5.074(4)	94.57(7)	5.197	1
Fergusonite-type	$TbNbO_4$	2.382	1.881	136.27	1.035	1.040	0.48	5.349(1)	11.036(9)	5.085(1)	94.62(3)	5.217	1
Fergusonite-type	$GdNbO_4$	2.394	1.889	135.06	1.035	1.053	0.48	5.374(3)	11.095(9)	5.106(5)	94.58	5.240	4
Fergusonite-type	$EuNbO_4$	2.407	1.884	134.89	1.036	1.066	0.48	5.395(1)	11.135(1)	5.116(1)	94.62(1)	5.253	1
Fergusonite-type	$SmNbO_4$	2.417	1.888	134.45	1.036	1.079	0.48	5.422(5)	11.178(9)	5.121(5)	94.69	5.272	4
Fergusonite-type	$PrNbO_4$	2.466	1.875	134.62	1.035	1.093	0.48	5.499(2)	11.342(7)	5.157(2)	94.57(5)	5.328	1
Fergusonite-type	$NdNbO_4$	2.447	1.879	129.09	1.034	1.109	0.48	5.467(1)	11.279(1)	5.146(1)	94.50(1)	5.307	2
Fergusonite-type	$CeNbO_4$	2.476	1.883	132.79	1.035	1.143	0.48	5.535(1)	11.399(1)	5.159(1)	94.60(1)	5.347	5
Fergusonite-type	$LaNbO_4$	2.505	1.874	121.41	1.032	1.160	0.48	5.565(1)	11.519(1)	5.202(1)	94.10(1)	5.383	2
Fergusonite-type	(As-rich) $YNbO_4$	2.374	1.808	46.94	1.012	1.024	0.39	5.179(1)	11.090(3)	5.118(1)	91.28(1)	5.149	6
Scheelite-type	$SmAsO_4$	2.427	1.697	26.14	1.007	1.079	0.335	5.066(1)	11.461(1)	5.066(1)	90.00	5.066	7
Scheelite-type	$CeNbO_4$	2.497	1.854	22.43	1.006	1.143	0.48	5.377(1)	11.595(1)	5.377(1)	90.00	5.377	8
Scheelite-type	$YNbO_4$	2.500	1.892	25.41	1.007	1.014	0.48	5.160	10.890	5.160	90.00	5.160	9

Note: References: [1] Keller (1962), [2] Tsunekawa et al. (1993), [3] Weitzel and Schröcke (1980), [4] Trunov and Kinzhibalo (1982), [5] Santoro et al. (1980), [6] this study, [7] Kang and Schleid (2006), [8] Skinner et al. (2004), [9] Komkov (1959).
* AV = angle variance and QE = quadratic elongation (Robinson et al. 1971).
† *c* refers to *b* in scheelite-type structures.

graphic data on synthetic fergusonite-type niobates with different cations in the A site (REE and Y). Using these data, we confirm a linear correlation between the average distance <A-O> and the ionic radius of the A-site cation ^{A}<r_i>, as first noted by Kinzhibalo et al. (1982): ^{A}<r_i> = 0.943*<A-O> (Å) – 1.2057 (R^2 = 0.97). The sample examined in the present study and published data on scheelite-type structures (with As or Nb at the B site) plot on the same trend (Fig. 3a). The only outliers are synthetic $PrNbO_4$ studied by Keller (1962) and scheelite-type fergusonite studied by Komkov (1959), who reported a rather unusual A-site occupancy for this natural sample, $Y_{0.85}Yb_{0.15}NbO_4$. With the above equation, Komkov's data give a calculated ionic radius of 1.15 Å, which is much closer to that of La. It is clear that deviation of this sample from the above trend results from the inadequacy of its chemical analysis.

Another interesting relationship was observed between the *a* lattice parameter and the mean ionic radius of the A-site cation. Fergusonite-type compounds define a linear trend with ^{A}<r_i> = 0.521*a (Å) – 1.7468 (R^2 = 0.98) because changes in A-site occupancy (with fixed B-site occupancy) have a very limited effect on the β angle. Scheelite-type polymorphs plot outside that trend and so does the As-rich monoclinic sample examined in this study (Fig. 3b). If we ignore the monoclinic distortion by averaging the *a* and *c* lattice parameters, the scheelite-type compounds with Nb in their B site plot along the trend (Fig. 3c), but not the As-rich sample. This deviation implies that the incorporation of As reduces the length of the *a* lattice parameter, or has an important effect on the β angle, thus reducing the magnitude of monoclinic distortion. This can be also seen in Figure 3d, where the AV value of Robinson et al. (1971) is plotted vs. ^{A}<r_i>: while monoclinic phases with light to medium rare-earth cations at the A site show a progressive decrease of the AV value with increasing ^{A}<r_i>, tetragonal phases show a much smaller distortion of the B tetrahedron, and so does the As-rich sample. Considering the fact that only about 25% of the B positions are occupied by As and that fergusonite-type structures undergo a phase transition to the scheelite-type structure with decreasing *T*, it is plausible that the presence of As reduces the temperature of the tetragonal-to-monoclinic transition. Therefore, in principle, it would be possible to expect that an increase in As content would lead to a change in symmetry from $I2/a$ to $I4_1/a$, the distortion being proportional to the As content. Clearly, experimental data on intermediate Nb-As compositions will be necessary to explore the compositional dependence of the monoclinic-to-tetragonal phase transition in fergusonite.

It is well known that increasing *P* leads to phase transitions from scheelite-type to fergusonite-type structures (Grzechnik et al. 2005) and from zircon-type to scheelite-type structures (Stubican and Roy 1963; Zhang et al. 2008). It has been also proposed that a wolframite-type phase is the post-fergusonite-type structure with increasing pressure (Li et al. 2004), whereas the scheelite to wolframite high-*P* phase transition has been predicted for $CaMoO_4$ and $CaWO_4$ by Nicol and Durana (1971) and confirmed by Errandonea et al. (2003). These phase transitions have been modeled by Fukunaga and Yamaoka (1979) and Bastide (1987) as a function of the ratio of the ionic radii of cations at both A and B sites and of the ionic radius of the anion. Recently, transformation from a zircon-to-scheelite structure and, at higher *P*, to a fergusonite-type structure has been described for $LuVO_4$ (Mittal et al. 2008).

Kolitsch and Holtstam (2004) reviewed the crystal chemistry of $REEXO_4$ compounds (with X = As, V, and P), which show both the monazite- and zircon-type topologies. Depending on the ionic radius of the lanthanide considered, for a fixed composition of the B site, the larger the REE^{3+} cation, the more stable the monazite-type structure. At the same time, an increase in size of the XO_4 group destabilizes the monazite structure in favor of the zircon-type structure. Loskutov et al. (1977) even proposed that an increase in ionic radius of the X cation ultimately leads to the stabilization of a scheelite structure and, for very large X, a wolframite-type structure. Interestingly, $SmAsO_4$ falls close to the region in which the structural topology of REE arsenates changes from that of monazite (REE = La, Ce, Pr, and Nd and REE = Pm-Lu, Y, and Sc; see Kolitsch and Holtstam 2004 and

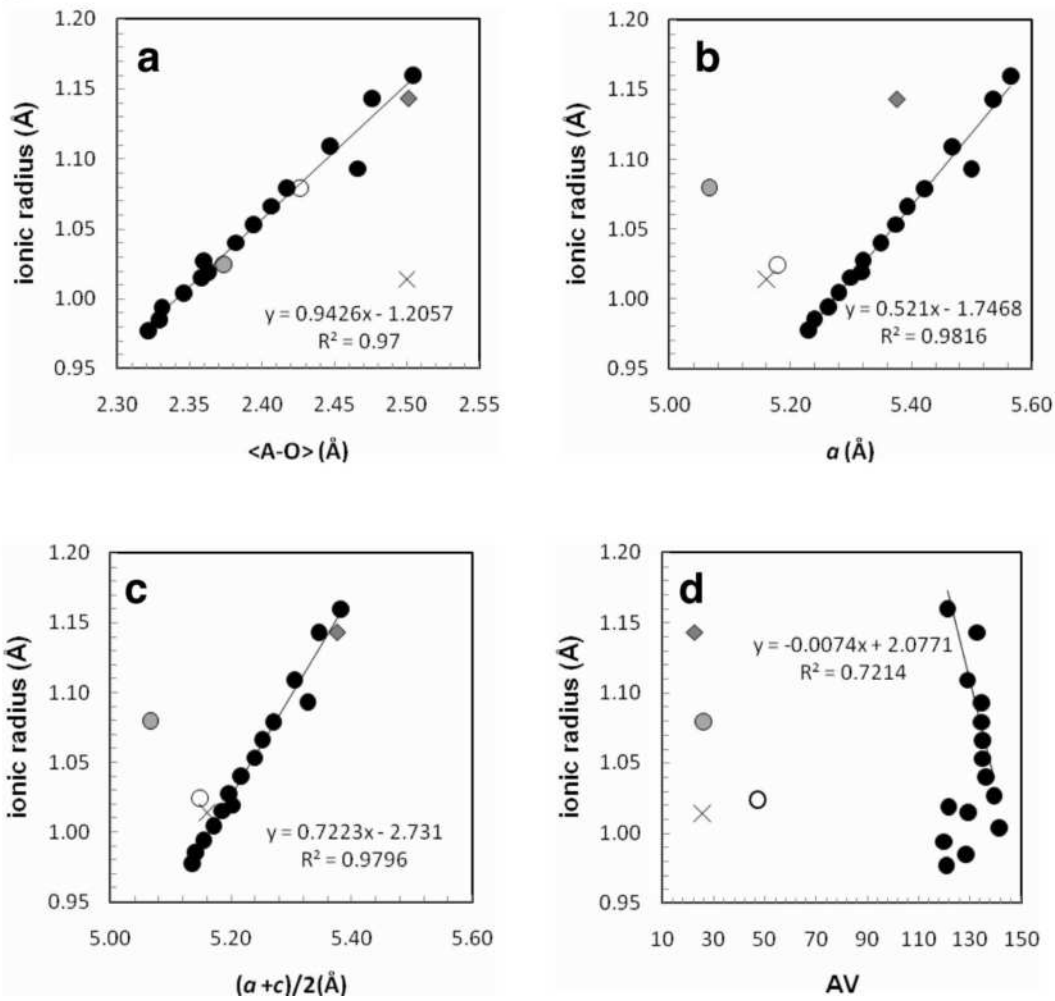

FIGURE 3. Relations between the average ionic radius at the A site and (**a**) the average bond distance at the A site, (**b**) *a* lattice parameter, (**c**) average *a*+*c* lattice parameter, and (**d**) angle-variance value (Robinson et al. 1971) for the studied sample (open circle), $SmAsO_4$ of Kang and Schleid (2006) (gray circle), T-fergusonite-(Ce) of Skinner et al. (2004) (gray diamond), T-fergusonite-(Y) of Komkov (1959) (cross) and synthetic fergusonite-type $REENbO_4$ with variying composition of the A site (references as in Table 5) (black circles).

references therein). According to Kang and Schleid (2006), scheelite-type structures are stabilized at high *P*, and become metastable at room *P*. However, scheelite-type $NdAsO_4$ has also been reported from room-*P* synthesis at 550 °C (Mazhenov et al. 1988).

In Figure 4, three ABO_4 structure types with different topologies but the same coordination for A and B cations (fergusonite-type, scheelite-type, and zircon-type) are compared. From a descriptive point of view, a shift along the *c* axis within (110) planes would change the zircon-type topology [as found in chernovite-(Y)] to the scheelite topology. The latter structure type can easily undergo a symmetry reduction to monoclinic by softer distortion. Figure 4 shows only the topologies stable at room *P* and *T*; the actual mechanism of the zircon-scheelite transformation at high pressure is much more complex and involves a change in coordination of the O atoms, which undergo a displacement of ca. 1 Å (Smirnov et al. 2008). Structural changes are required to effect a transition to the fergusonite topology, as can be seen from the results of Mittal et al. (2008), who observed a negligible volume change during the scheelite-to-fergusonite phase transition, and proposed that it is a second-order displacive phase transition. In addition, Kolitsch and Holtstam (2004) proposed that the presence of impurities (Ca, Th, U, and Si) can stabilize one or the other

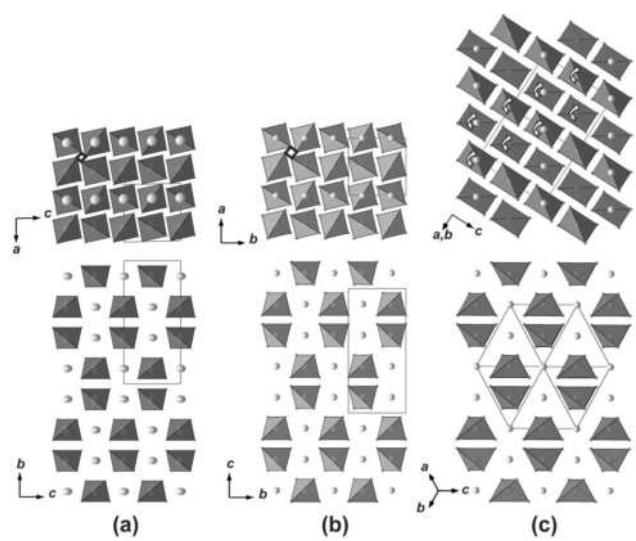

FIGURE 4. Sketch comparing the structures of fergusonite topology (**a**), scheelite topology in two different orientations (**b**), and zircon topology (**c**). The open squares in the fergusonite and scheelite topologies help in visualizing the tetragonal-to-monoclinic deformation. White spheres are A sites. Tetrahedra are B sites. The arrows in **c** show how a differential shift along [001](110) relates the zircon and scheelite topologies.

polymorph. The sample studied in the present work contains all of the above elements, which may explain the stability of the fergusonite structure relative to the scheelite structure.

To conclude, although we cannot rule out the possibility that a complete series of scheelite-type compounds involving the As-for-Nb substitution exists, it is highly probable that there is at least one change in topology across that series, controlled mainly by atomic substitutions in the B site. Paraniite-(Y) [$Ca_2Y(AsO_4)(WO_4)_2$], which is also present at Mount Cervandone and may be viewed as an intermediate member of the solid solution between scheelite and chernovite-(Y), has an overall scheelite topology, but a tripled lattice periodicity along [001] owing to cation ordering in the symmetrically non-equivalent B sites along the *c* axis. We are conducting a detailed study of chernovite-(Y) samples from the same locality to constrain the chemical variations and possible changes in symmetry in naturally occurring Y arsenates.

Acknowledgments

We thank the fruitful comments of W. Crichton, an anonymous reviewer, and Associate Editor A. Chakhmouradian that helped to improve the manuscript. We also thank R. Carampin of CNR-IGG Padova for access to the WDS electron microprobe facility and R. Gastoni of CNR-IGG Pavia for sample preparation. Fernando Cámara was supported by funding by CNR-IGG through the project TAP01.004.002. Fabrizio Nestola was supported by funding by MIUR PRIN 2006047943 to A. Dal Negro.

References cited

Bastide, J.P. (1987) Systématique simplifiée des composés ABX_4 (X = O^{2-}, F^-) et evolution possible de leurs structures cristallines sous pression. Journal of Solid State Chemistry, 71, 115–120.

Bedlivy, D. and Mereiter, K. (1982) Structure of α-$BiAsO_4$ (rooseveltite). Acta Crystallographica, B38, 1559–1561.

Chashka, A.I. and Marchenko, Y.A. (1977) A new rare-earth niobate from carbonatites. Geologiya i Geofizika, no. 4, 141–143 (in Russian). (Not seen, cited in M. Fleischer and J. Jambor, Eds., New Minerals Names, American Mineralogist, 62, 395–397.)

Crichton, W.A. and Grzechnik, A. (2004) Crystal structure of calcium molybdate, $CaMoO_4$, a scheelite-type to fergusonite-type transition in powellite at $P > 15$ GPa. Zeitschrift für Kristallographie, 219, 337–338.

Dal Piaz, G. (1975) La val Devero ed i suoi minerali. Memorie Istituto di Geologia dell' Università di Padova, Vol. X, Società Cooperativa Tipografica, Padova.

Demartin, F. and Gramaccioli, C.M. (2008) The crystal structure of cervandonite-(Ce), an interesting example of $As^{3+} \rightarrow Si$ diadochy. The Canadian Mineralogist, 46, 423–430.

Demartin, F., Gramaccioli, C.M., and Pilati, T. (1994) Paraniite-(Y), a new tungstate arsenate mineral from Alpine fissures. Schweizerische Mineralogische Petrographische Mitteilungen, 74, 155–160.

Errandonea, D., Somayazulu, M., and Häusermann, D. (2003) Phase transitions and amorphization of $CaWO_4$ at high pressure. Physica Status Solidi (b), 235, 162–169.

Errandonea, D., Pellicer-Porres, J., Manjón, F.J., Segura, A., Ferrer-Roca, Ch., Kumar, R.S., Tschauner, O., Rodríguez-Hernández, P., López-Solano, J., Radescu, S., Mujica, A., Muñoz, A., and Aquilanti, G. (2005) High-pressure structural study of the scheelite tungstates $CaWO_4$ and $SrWO_4$. Physical Review B, 72, 174106.

Fukunaga, O. and Yamaoka, S. (1979) Phase transformations in ABO_4 type compounds under high pressure. Physics and Chemistry of Minerals, 5, 167–177.

Farrugia, L.J. (1999) WinGX suite for small-molecule single-crystal crystallography. Journal of Applied Crystallography, 32, 837–838.

Galliski, M.A., Marquez-Zavalia, M.F., Cooper, M.A., Cerny, P., and Hawthorne, F.C. (2001) Bismutotantalite from northwestern Argentina: description and crystal structure. The Canadian Mineralogist, 39, 103–110.

Goldin, B.A., Yushkin, N.P., and Fishmin, M.V. (1967) A new yttrium mineral, chernovite. Zapiski Vserossiiskovo Mineralogicheskovo Obshchestva, 96, 699–704 (in Russian).

Gorzhevskaya, S.A., Sidorenko, G.A., and Smorchkov, I.E. (1961) A new modification of fergusonite: β-fergusonite. Geologiya Mestorozhdenii Redkikh Elementov, 9, 28–29 (in Russian).

Graeser, S. (1966) Asbecasit und cafarsit, zwei neue mineralien aus dem Binnatal (Kt. Wallis). Schweizerische Mineralogische Petrographische Mitteilungen, 46, 367–375.

Graeser, S. and Albertini, C. (1995) Wannigletscher und Conca Cervandone. Lapis, 20, 41–64.

Graeser, S. and Schwander, H. (1987) Gasparite-(Ce) and monazite-(Nd): two new minerals to the monazite group from the Alps. Schweizerische Mineralogische Petrographische Mitteilungen, 67, 103–113.

Graeser, S., Schwander, H., Demartin, F., Gramaccioli, C.M., Pilati, T., and Reusser, E. (1994) Fetiasite (Fe^{2+}, Fe^{3+}, $Ti)_3O_2[As_2O_5]$, a new arsenite mineral: Its description and structure determination. American Mineralogist, 79, 996–1002.

Grzechnik, A., Friese, K., Dmitriev, V., Weber, H.P., Gesland, J.Y., and Crichton, W.A. (2005) Pressure-induced tricritical phase transition from the scheelite structure to the fergusonite structure in $LiLuF_4$. Journal of Physics: Condensed Matter, 17, 763–770.

Guastoni, A., Pezzotta, F., and Vignola, P. (2006) Characterization, paragenesis and genetic inferences of arsenates, sulfates and vanadates of Fe, Cu, Pb, Zn from Mount Cervandone (Western Alps, Italy). Periodico di Mineralogia, 76, 141–150.

Hazen, R.M., Finger, L.W., and Mariathasan, J.W.E. (1985) High-pressure crystal chemistry of scheelite-type tungstates and molybdates. Journal of Physics and Chemistry of Solids, 46, 253–263.

Hori, H., Kobayashi, T., Miyawaki, R., Matsubara, S., Yokoyama, K., and Shimizu, M. (2006) Iwashiroite-(Y), $YTaO_4$, a new mineral from Suishoyama, Kawamata Town, Fukushima Prefecture, Japan. Journal of Mineralogical and Petrological Sciences, 101, 170–177.

Kang, D.H. and Schleid, T. (2006) Einkristalle von $Sm[AsO_4]$ im scheelit-typ. Zeitschrift für Anorganische und Allgemeine Chemie, 632, 2147.

Keller, C. (1962) Ueber ternaere oxide der niobs und tantals vom typ ABO_4. Zeitschrift für Anorganische und Allgemeine Chemie, 318, 89–106.

Kinzhibalo, L.N., Trunov, V.K., Evdokimov, A.A., and Krongauz, V.G. (1982) Refinement of the crystal structure of fergusonite. Soviet Physics-Crystallography, 27, 22–25.

Kolitsch, U. and Holtstam, D. (2004) Crystal chemistry of $REE\mathit{X}O_4$ compounds (X = P, As, V). II. Review of $REE\mathit{X}O_4$ compounds and their stability fields. European Journal of Mineralogy, 16, 117–126.

Komkov, A.I. (1959) The structure of natural fergusonite and of a polymorphic modification. Kristallografiya, 4, 836–841 (in Russian).

Krstanović, I. (1965) Redetermination of oxygen parameters in xenotime, YPO_4. Zeitschrift für Kristallographie, 121, 315–316.

Li, S., Ahuja, R., and Johansson, B. (2004) Wolframite: The post-fergusonite phase in $YLiF_4$. Journal of Physics: Condensed Matter, 16, S983–S988.

Liu, L. (1979) High-pressure phase transformations in baddeleyite and zircon, with geophysical implications. Earth and Planetary Science Letters, 44, 390–395.

Loskutov, V.V., Vorobzhanskaya, É.V., and Liberman, Z.A. (1977) Structural diagram of compounds ABO_4. Soviet Physic Crystallography, 22, 726–728.

Manjon, F.J. and Errandonea, D. (2009) Pressure-induced structural phase transitions in materials and Earth sciences. Physica Status Solidi (b), 246, 9–31.

Mazhenov, N.A., Nurgaliev, B.Z., and Muldakhmetov, K.Z. (1988) Scheelite modification of neodymium arsenate. Izvestiya Akademii Nauk SSSR, Neorganicheskie Materialy, 24, 1163–1165 (in Russian).

Mittal, R., Garg, A.B., Vijayakumar, V., Achary, S.N., Tyagi, A.K., Godwal, B.K., Busetto, E., Lausi, A., and Chaplot, S.L. (2008) Investigation of the phase stability of $LuVO_4$ at high pressure using powder X-ray diffraction measurements and lattice dynamical calculations. Journal of Physics: Condensed Matter, 20, 075223.

Mooney, R.C.L. (1948) Crystal structure of tetragonal bismuth arsenate, $BiAsO_4$. Acta Crystallographica, 1, 163–165.

Mrose, M.E. and Rose Jr., J. (1961) Behierite, (Ta, Nb)BO_4, a new mineral from Manjaka, Madagascar. Geological Society of America, Abstracts 1961, Annual Meetings, p. 111A.

Nicol, M. and Durana, J.F. (1971) Vibrational expectra of $CaMoO_4$ and $CaWO_4$ at high pressures. Journal of Chemical Physics, 54, 1436–1440.

Pouchou, J.L. and Pichoir, F. (1985) "PAP" (phi-rho-z) procedure for improved quantitative microanalysis. In J.T. Armostrong, Ed., Microbeam Analysis, p. 104–106. San Francisco Press, California.

Reid, A.F. and Ringwood, A.E. (1969) Newly observed high pressure transformations in Mn_3O_4, $CaAl_2O_4$, and $ZrSiO_4$. Earth and Planetary Science Letters, 6, 205–208.

Robinson, K., Gibbs, G.V., and Ribba, P.H. (1971) Quadratic elongation: A quantitative measure of distortion in coordination polyhedra. Science, 172, 567–570.

Santoro, A., Marezio, M., Roth, R.S., and Minor, D. (1980) Neutron powder diffraction study of the structures of $CeTaO_4$, $CeNbO_4$, and $NdTaO_4$. Journal of Solid State Chemistry, 35, 167–175.

Scott, H.P., Williams, Q., and Knittle, E. (2002) Ultralow compressibility silicate without highly coordinated silicon. Physical Review Letters, 88, 015506.

Sheldrick, G.M. (1997) Programs for Crystal Structure Analysis (Release 97-2). Institüt für Anorganische Chemie der Universität, Göttingen, Germany.

——— (1998) SHELXTL/SADABS. Version 5.1. Bruker AXS, Madison, Wisconsin.

Skinner, S.J., Brooks, I.J.E., and, Munnings, C.N. (2004) Tetragonal $CeNbO_4$ at 1073 K in air and in vacuo. Acta Crystallographica, C60, i37–i39.

Smirnov, M.B., Mirgorodsky, A.P., Kazimirov, V.Y., and Guinebretière, R. (2008) Bond-switching mechanism for the zircon-scheelite phase transition. Physical Review B, 78, 094109.

Strada, M. and Schwendimann, G. (1934) La struttura cristallina di alcuni fosfati ed arseniati di metalli trivalenti. II. Arseniato e fosfato di ittrio. Gazzetta Chimica Italiana, 64, 662–674.

Stubican, V.S. and Roy, R. (1963) High-pressure scheelite-structures polymorphs of rare-earth vanadates and arsenates. Zeitschrift für Kristallographie, 119, 90–97.

Sugitani, Y. and Nagashima, K. (1975) Flux growth of $YNbO_4$. Mineralogical Journal, 8, 66–71.

Troitzsch, U., Christy, A.G., and Ellis, D.J. (2007) Synthesis of zirconium titanate with an ordered M-fergusonite (beta) structure. Journal of Solid State Chemistry, 180, 2885–2895.

Trunov, V.K. and Kinzhibalo, L.N. (1982) The change of structures $LnNbO_4$ in the lanthanoid series. Doklady Akademii Nauk SSSR, 263, 348–351 (Kristallografiya, 27, 43–48).

Tsunekawa, S., Kamiyama, T., Sasaki, K., Asano, H., and Fukuda, T. (1993) Precise structure analysis by neutron diffraction for $RNbO_4$ and distortion of NbO_4 tetrahedra. Acta Crystallographica, A49, 595–600.

Weitzel, H. and Schröcke, H. (1980) Kristallstrukturverfeinerungen von euxenit, $Y(Nb_{0.5}Ti_{0.5})_2O_6$ und M-fergusonit, $YNbO_4$. Zeitschrift für Kristallographie, 152, 69–82.

Wilson, A.C.J. (1992) International Tables for Crystallography, Volume C. Kluwer Academic Publishers, Dordrecht.

Wolten, G.M. (1967) The structure of the M'-Phase of $YTaO_4$, a third Fergusonite polymorph. Acta Crystallographica, 23, 939–944.

Wolten, G.M. and Chase, A.B. (1967) Synthetic fergusonites and a new polymorph of yttrium tantalate. American Mineralogist, 52, 1536–1541.

Zhang, F.X., Lang, M., Ewing, R.C., Lian, J., Wang, Z.W., Hu, J., and Boatner, L.A. (2008) Pressure-induced zircon-type to scheelite-type phase transitions in $YbPO_4$ and $LuPO_4$. Journal of Solid State Chemistry, 181, 2633–2638.

Manuscript received March 11, 2009
Manuscript accepted November 10, 2009
Manuscript handled by Anton Chakhmouradian